Synthesis, Crystal Structure and Fluorescence Property of a Zinc(II) Coordination Polymer with a Theoretical Calculatio①

WANG Wen-Qian[a, b] CHEN Jun[c]
WANG Shuai-Hua[b] WU Shao-Fan[b②]

[a] (*College of Chemistry and Chemical Engineering, Fujian Normal University, Fuzhou* 350117, *China*)

[b] (*Key Laboratory of Optoelectronic Materials Chemistry and Physics, Fujian Institute of Research on the Structure of Matter, Chinese Academy of Sciences, Fuzhou* 350002, *China*)

[c] (*School of Ecological Environment and Urban Construction, Fujian University of Technology, Fuzhou* 350118, *China*)

ABSTRACT We have designed and synthesized a new luminescent coordination polymer $[Zn_2(NO_3)(NCP)_3(H_2O)_3]_n \cdot 2nH_2O$ (**1**, HNCP = 2-(2-carboxyphenyl) imidazo-[4,5-f]-1,10-phenanthroline) under hydrothermal conditions, which has been structurally characterized by single-crystal X-ray diffraction analyses. **1** crystallizes in monoclinic, space group $P2_1/n$, with a = 13.7748(3), b = 19.2651(4), c = 19.9543(4) Å, β = 95.339(2)°, V = 5272.35(19) Å^3, $C_{60}H_{39.73}N_{13}O_{13.33}Zn_2$, M_r = 1286.80, D_c = 1.621 g/cm^3, Z = 4, μ(Mo$K\alpha$) = 2.118, F(000) = 2629, the final R = 0.0598 and wR = 0.1483. In **1**, the organic ligand NCP^- displays two different bridging modes to connect adjacent Zn(II) ions into a 1D chain along the *c*-direction. Photoluminescent analyses reveal that **1** exhibits a strong green emission with a fluorescent lifetime of 5.57 ns. The first-principle calculation results show that the luminescence mainly originates from ligand-centered charge transition.

Keywords: hydrothermal method, crystal structure, luminescence, theoretical calculation;
DOI: 10.14102/j.cnki.0254–5861.2011–2769

1 INTRODUCTION

Coordination polymers (CPs) are assembled by metal atoms or metal clusters as connecting nodes, and organic bridging ligands as linkers[1]. The synthesis of new CPs has received considerable attention in recent years. CPs as a new type of structurally diversified and unique characteristic materials in catalysis[2-4], sensing[5], gas storage and separation[6, 7] luminescence[8-10], and supercapacitor[11]. Meanwhile, CPs also exhibit even more unexpected applications in luminescent performance, with deeper mechanism research, such as metal-centered charge transfer, metal-to-ligand charge transfer, ligand-centered charge transfer and ligand-to-metal charge transfer[12-14]. Generally, luminescent coordination polymers choose rare-earth metal, but recently, CPs based on nonluminescent zinc ions have attracted particular attention for their low expense and biocompatibility[15-17]. Zn(II) ion as d^{10} metal ion possesses various coordination numbers, and can coordinate with O and N atoms[18-20]. At the same time, structural and functional design is also a research feature of CPs, and large conjugated ligands form excellent fluorescent luminescent CPs[21]. In our research, we chose a large conjugated organic molecule 2-(2-carboxyphenyl) imidazo (4,5-*f*) (1,10) phenanthroline (HNPC) as the ligand because it possesses richer electronic behaviors and are usually used to construct luminescent compounds[22]. Consequently, we design and synthesize a new Zn(II) coordination polymer $[Zn_2(NO_3)(NCP)_3(H_2O)_3]_n \cdot 2nH_2O$ by hydrothermal reaction. Pertinent crystal data and structure refinement results for **1** are summarized in Table S1, and selected bond lengths and bond angles are listed in Table S2. Structural analysis shows that NCP^- in **1** displays two different bridging fashions (Scheme 1). In addition, the luminescent property of **1** was investigated in the solid state at room temperature. Moreover, the coordina-

Received 19 February 2020; accepted 12 May 2020 (**CCDC 1977517**)

① This work was supported by the National Key Research Project (No. 2017YFB1104504), the Financial Support of Fujian Province (2017J05017 and 2017H0043) and the National Natural Science Foundation of China (No. 51872287)

② Corresponding author. Wu Shao-Fan. E-mail: sfwu@fjirsm.ac.cn

tion polymer has green fluorescence under 380 nm light excitation, and we use the first-principle calculation to reveal the emitting mechanism of **1**.

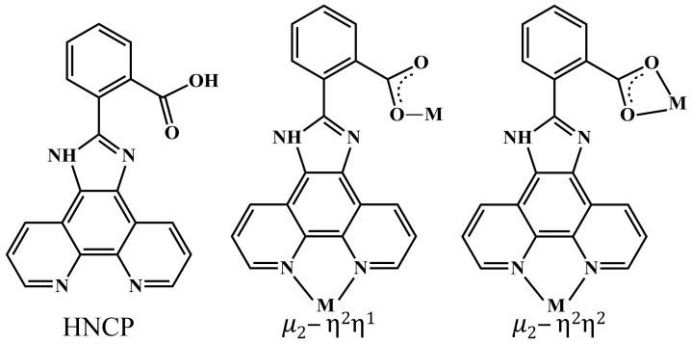

Scheme 1. Structural formula of HNCP and two bridging modes of NCP^- ligand in 1

2 EXPERIMENTAL

2. 1 Materials and instruments

All chemicals and solvents were used without further purification. Powder X-ray diffraction (PXRD) patterns were collected on a Rigaku Miniflex 600 diffractometer using Cu$K\alpha$ radiation at 40 kV and 40 mA in the range of $5 \leqslant 2\theta \leqslant 60°$. The FT-IR spectra were obtained on a Perkin-Elmer spectrum in the range of 4000～400 cm^{-1} using KBr disks. The thermogravimetric analysis (TGA) was determined by NETZSCH STA 449F3 Jupiter thermo-gravimetric analyzer, with the sample heated in an alumina crucible in a nitrogen atmosphere at a heating rate of 10 K/min. Luminescence excitation and emission spectra of the samples were using a 500 W Xenon lamp as excitation source obtained on an Edinburgh FLS1000 spectrophotometer.

2. 2 Synthesis

A mixture of ligand HNCP (15 mg, 0.15 mmol), $Zn(NO_3)_2{\cdot}6H_2O$ (44.6 mg, 0.15 mmol) and KOH (5.6 mg, 0.1 mmol) in distilled water (10 mL) was sealed into a 25 mL poly(tetrafluoroethylene)-lined stainless-steel container under autogenous pressure and then heated at 140 ℃ for 3 days and cooled to 30 ℃ at a rate of 2.5 ℃·h^{-1}. Orange block crystals suitable for X-ray analyses were obtained, washed with distilled ethanol and dried in air. Yield: 30% (based on HNCP) for **1**. Anal. Calcd. for $C_{60}H_{39.73}N_{13}O_{13.33}Zn_2$: C, 56.00; H, 3.11; N, 14.15%. Found: C, 56.36; N, 3.13; H, 14.25%. IR (KBr pellet, cm^{-1}): 3515 m, 3415 s, 3075 m, 1615 s, 1556 w, 1510 m, 1375 s, 1247 w, 1141 w, 1083 m, 1029 s, 970 m, 931 m, 735 s, 648 m.

2. 3 Single-crystal structure determination

Single crystals of **1** suitable for X-ray analyses were stuck to a fiberglass. Data collections were performed on a Rigaku Saturn-70 CCD diffractometer at 293 K. All diffractometers were equipped with graphite-monochromated Mo-$K\alpha$ radiation (λ = 0.71073 Å). The intensity data sets were collected with the ω scan technique and reduced by CrystalClear software. A total of 46809 reflections were collected in the range of $1.74 \leqslant \theta \leqslant 27.50°$, of which 11740 were independent (R_{int} = 0.0756) and 8714 were observed ($I > 2\sigma(I)$). The structures were solved by direct methods with the SHELXTL (version 5) crystallographic software package and refined by full-matrix least-squares refinement on F^2. Non-hydrogen atoms were located by difference Fourier maps and subjected to anisotropic refinement. The hydrogen atoms of water molecules except those belonging to disordered ones were located in difference Fourier syntheses and refined with O–H distances restrained to a target value of 0.85 Å and $U_{iso}(H) = 1.5U_{eq}(O)$, and other hydrogen atoms were added according to theoretical models. The final R = 0.0598, wR = 0.1483 ($w = 1/[\sigma^2(F_o^2) + (0.0731P)^2 + 9.1842P]$, where $P = (F_o^2 + 2F_c^2)/3$), $(\Delta/\sigma)_{max}$ = 0.001, S = 1.112, $(\Delta\rho)_{max}$ = 1.978 and $(\Delta\rho)_{min}$ = –0.879 e·Å^{-3}. Selected bond lengths and bond angles are listed in Table 1.

3 RESULTS AND DISCUSSION

3. 1 Structure description

X-ray crystallographic analysis shows that **1** crystallizes in monoclinic space group $P2_1/n$ and features a 1D chain structure. Each asymmetric unit contains two crystallographically independent Zn(II) centers (Zn(1) and Zn(2)), three NCP^- ligands (labeled as L_I, L_{II}, L_{III}), two coordinated water molecules and three lattice water molecules. The

coordination geometry around the Zn(1) ion can be described as a distorted square pyramidal geometry. As illustrated in Fig. 1, one oxygen atom (O(5W)) from water molecule, two nitrogen atoms (N(11A), N(12A)) and another oxygen atom from two symmetry-related of L_I ligands constitute the equatorial plane, while the axial position is filled by a carboxylate O(21) atom from L_{II}, whereas the Zn(2) center is six-coordinated and resides in a distorted octahedral environment with four nitrogen atoms (N(21), N(22), N(31), N(32)) and two oxygen atoms (O(31B), O(32B)) from two crystallographically independent NCP^- ligands (L_{II} and L_{III}). The N(22), N(31), O(31B) and O(32B) atoms constitute the equatorial plane, while N(21) and N(32) atoms occupy the apical positions with the axial angle N(21)–Zn(2)–N(32) of 169.36(9)° deviating from the ideal angle of 180°. All the Zn–N and Zn–O distances of 1.808(5)～2.405(11) and 1.765(4)～2.251(2) Å are in the normal ranges, respectively[23, 24]. Two different bridging styles of NCP^- ligands have been observed in **1**: the L_I and L_{II} ligands display similar coordination mode: μ_2-$\eta^2\eta^1$, while the L_{II} ligand adopts a μ_2-$\eta^2\eta^2$ mode (Scheme 1). The L_I and L_{II} ligands connect adjacent Zn(1) and Zn(2) ions into a tetranuclear zinc(II) cluster (Fig. 2(b)). Then, the paratactic L_{III} ligands, acting as double linkers, bridge neighboring zinc(II) clusters to generate a 1D chain along the *c*-direction (Fig. 2(c)). As the NCP^- ligand owns large conjugate system, $\pi\cdots\pi$ interactions exist between adjacent organic ligands in the 1D chains of **1**. There exist intrachain hydrogen bonds among the NCP^- ligand, two water molecules and NO_3^- ion with the H-band distance of 2.665(10)～2.897(4) Å (Fig. S1). These chains stack together in an ···ABAB··· fashion along the *b* axis (Fig. S2).

Table 1. Selected Bond Lengths (Å) and Bond Angles (°) for 1

Bond	Dist.	Bond	Dist.
Zn(1)–O(21)	1.879(3)	Zn(2)–O(31)#2	2.251(2)
Zn(1)–O(11)	1.765(4)	Zn(2)–N(22)	2.138(2)
Zn(1)–N(11)#1	1.808(5)	Zn(2)–N(31)	2.129(3)
Zn(1)–N(12)#1	2.41(1)	Zn(2)–N(21)	2.103(2)
Zn(1)–O(5W)	2.864(4)	Zn(2)–N(32)	2.138(2)
Zn(2)–O(32)#2	2.152(2)		
Angle	(°)	Angle	(°)
O(21)–Zn(1)–N(12)#1	111.1(2)	N(31)–Zn(2)–O(32)#2	156.09(9)
O(21)–Zn(1)–O(5W)	101.8(2)	N(31)–Zn(2)–O(31)#2	99.94(9)
O(11)–Zn(1)–O(21)	113.1(1)	N(31)–Zn(2)–N(22)	102.3(1)
O(11)–Zn(1)–N(11)#1	112.5(2)	N(31)–Zn(2)–N(32)	77.9(1)
O(11)–Zn(1)–O(5W)	98.3(2)	N(21)–Zn(2)–O(32)#2	94.84(9)
O(5W)–Zn(1)–N(11)#1	164.6(2)	N(21)–Zn(2)–O(31)#2	95.00(9)
O(11)–Zn(1)–N(12)#1	120.8(3)	N(21)–Zn(2)–N(22)	78.86(9)
N(11)#1–Zn(1)–O(21)	117.8(1)	N(21)–Zn(2)–N(31)	99.9(1)
N(11)#1–Zn(1)–N(12)#1	77.2(3)	N(21)–Zn(2)–N(32)	169.39(9)
N(12)#1–Zn(1)–O(5W)	89.3(3)	N(32)–Zn(2)–O(32)#2	90.73(9)
O(32)#2–Zn(2)–O(31)#2	59.85(9)	N(32)–Zn(2)–O(31)#2	95.60(9)
N(22)–Zn(2)–O(32)#2	98.98(9)	N(32)–Zn(2)–N(22)	91.37(9)
N(22)–Zn(2)–O(31)#2	157.68(9)		

Symmetry codes for **1**: #1: 1 – *x*, 1 – *y*, 1 – *z*; #2: 1 – *x*, 1 – *y*, 2 – *z*

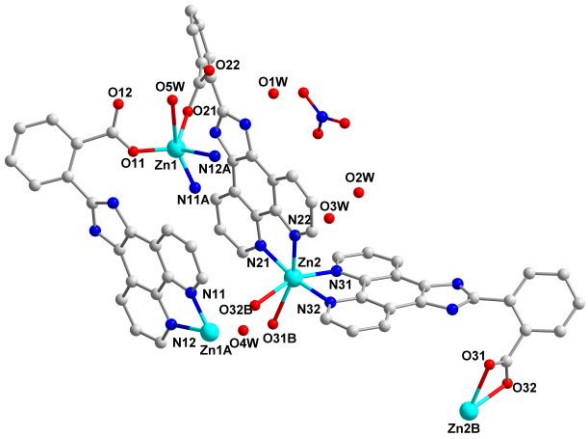

Fig. 1. Asymmetric unit and coordination geometry of Zn(II) ions in 1. Symmetry codes: A: –*x* + 1, –*y* + 1, –*z* + 1, B: –*x* + 1, –*y* + 1, –*z* + 2. Hydrogen atoms have been omitted for clarity

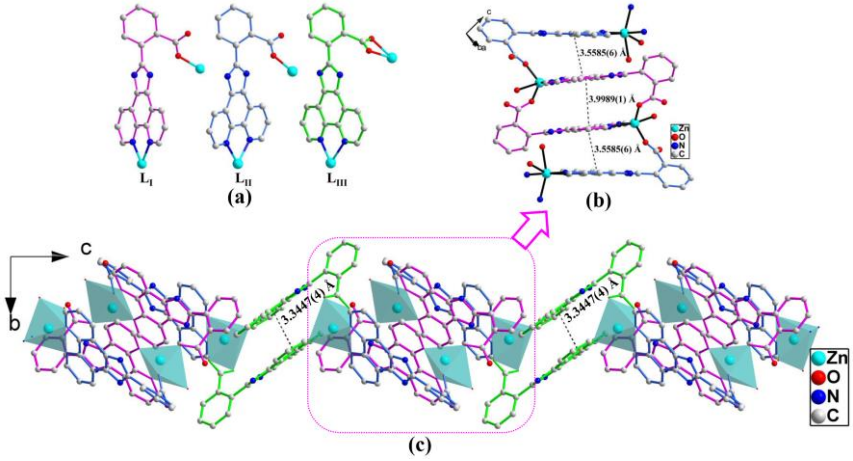

Fig. 2. (a) Three crystallographically independent NCP^- ligands (labeled as L_I, L_{II} and L_{III}). (b) Tetranuclear zinc(II) cluster. (c) 1D chain of 1 along the *c*-direction. Hydrogen atoms have been omitted for clarity

3. 2 Powder X-ray diffraction and thermal analysis

The experimental powdered X-ray diffraction (PXRD) pattern of **1** agrees well with the simulated one based on the single-crystal X-ray data (Fig. S3), indicating that **1** is in a pure phase. Thermogravimetric analyses (TGA) curves (Fig. S4) show that there is no obvious weight loss below 100 ℃. With continuous heating, the weight loss of 2.8% from 100 to 250 ℃ corresponded to the release of two water molecules. Further heating led to the decomposition of organic ligands, and the loss of other three water molecules.

3. 3 Luminescent properties

In order to decrease the influence of self-aggregation, the luminescence of free ligand HNCP was investigated in degassed dichloromethane at room temperature (Fig. 3(a)). The HNPC shows a broad emission centred at ~400 nm upon the excitation wavelenghth of 270 nm, and the overall emission is located in the blue region, as illustrated by the CIE (CIE = Commission International de l'Echairage) chromaticity coordinates (0.198, 0.147) of the emission spectra in Fig. 3(b). Such emissions observed in the free ligand HNPC can be assigned to the typical ligand-centered transitions. The solid-state luminescence of polymer **1** was also investigated at room temperature. As depicted in Fig. 3(a), Polymer **1** displys a dominant emission band at ~500 nm when excited by 380 nm light. The overall emission is located in the green region with CIE chromaticity coordinate of (0.242, 0.385). Compared with free ligand, emission band of **1** displays significant red-shift, which might be attributed to different charge transfer in HNCP and **1**. Moreover, the emission decay time of **1** is 5.57 ns (λ_{em} = 500 nm, λ_{ex} = 380 nm) (Fig. S5), indicating that **1** has fluorescence characteristic.

3. 4 Theoretical calculation

To understand better the photoluminescent mechanism, the optimized structure of **1** was theoretically calculated by evaluation of the density of states (DOS). The calculation was

performed with the CASTEP code based on density functional theory with a plane-wave expansion of the wave functions. The calculated absorption edge value of **1** is 2.34 eV, which is similar with the measured one (2.77 eV) from optical absorption spectra (Fig. S6). As illustrated in Fig. 4, the top of the valence bands (VBs) mainly results from the p-π orbitals of NCP^- and a limited contribution of *d* orbitals of Zn(II) ions, while the CBs between energy 2 and 4 eV is almost contributed by p-π* antibonding orbitals of the NCP^- ligands. Theoretically speaking, ligand-to-ligand (LLCT) and metal-to-lignad charge transfer (MLCT) coexists in the absorption transition of **1**. Therefore, the emission peak at ~500 nm should be mainly attributed to the interligand π-π* transition of NCP^- ligand, in accordance with the other NCP^--based complexes[25]. The contribution of MLCT is comparatively limited. Both experimental and theoretical results consistently support the idea that the interligand charge transition in **1** presents a dominating contribution. This may be the reason why the emission band of **1** displays significant red-shift compared with HNCP ligands.

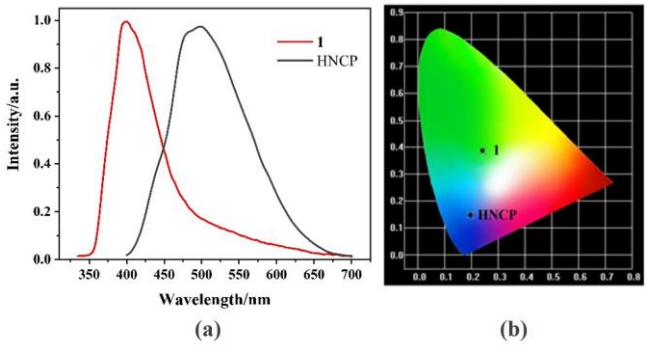

Fig. 3. (a) Emission spectra of 1 (λ_{ex} = 380 nm) in the solid state and HNCP (λ_{ex} = 270 nm) in dichloromethane. (b) CIE chromaticity diagram of 1 and HNCP

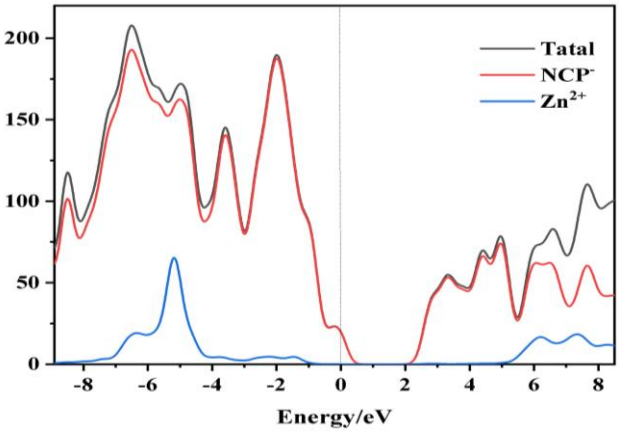

Fig. 4. Ttotal and partial DOS of 1 with the position of the Ferm level set at 0 eV

4 CONCLUSION

In summary, we have successfully prepared a novel 1D NCP^--based Zn(II) coordination polymer $[Zn_2(NO_3)(NCP)_3(H_2O)_3]_n$ $2nH_2O$ (**1**) using a hydrothermal method. Interestingly, the organic ligand NCP^- displays two different bridging modes to connect adjacent Zn(II) ions into a 1D chain along the *c*-direction. Furthermore, photoluminescent spectra demonstrate that **1** might be a good candidate for an efficient green emission material.

REFERENCES

(1) Kitagawa, S.; Kitaura, R.; Noro, S. Functional porous coordination polymers. *Angew. Chem. Int. Edit.* **2004**, 43, 2334–2375.

(2) Carraro, F.; Chapman, K.; Chen, Z. J.; Dincă, M.; Easun, T.; Eddaoudi, M.; Farha, O.; Forgan, R.; Gagliardi, L.; Haase, F.; Harris, D.; Kitagawa, S.; Knichal, J.; Lamberti, C.; Lee, J. M.; Leus, K.; Li, J.; Lin, W. B.; Lloyd, G.; Long, J. R.; Lu, C.; Ma, S. Q.; McHugh, L.; Perez, J. P. H.; Ranocchiari, M.; Rosi, N.; Rosseinsky, M.; Ryder, M. R.; Ting, V.; van der Veen, M.; Van Der Voort, P.; Volkmer, D.; Walsh, A.; Woods, D.; Yaghi, O. M.

Catalysis in MOFs: general discussion. *Faraday Discuss*. **2017**, 201, 369–394.

(3) Miao, C. L. Design and construction of a 2D Pb-II coordination polymer as a multi-response luminescent sensor for Fe^{3+}, $Cr_2O_7^{2-}$, and TNP. *J. Mol. Struct.* **2019**, 1193, 286–293.

(4) Zhu, Z. Q.; Tao, Y. F.; Jiang, Y. S.; Zhang, L. Y.; Xu, J. N.; Wang, L.; Fan, Y. Two scandium coordination polymers: rapid synthesis and catalytic properties. *CrystEngcomm.* **2019**, 21, 5261–5268.

(5) Lu, J. F.; Zhao, J.; Zhao, C. B.; Yu, X. H.; Soumendra, K. R.; Yue, S. Y.; Li, L.; Zhou, K.; Jin, Li. X.; Ge, H. G. A Chinese lantern-like 2D Cu(II) coordination polymer constructed by bis-imidazole and dicarboxylate Co-ligands: synthesis, crystal structure and photocatalytic activity. *Chin. J. Struct. Chem.* **2020**, 39, 321–328.

(6) Li, J. R.; Kuppler, R. J.; Zhou, H. C. Selective gas adsorption and separation in metal-organic frameworks. *ChemInform*. **2009**, 38, 1477–1504.

(7) Salunkhe, R. R.; Kamachi, Y.; Torad, N. L.; Hwang, S. M.; Sun, Z. Q.; Dou, S. X.; Kim, J. H.; Yamauchi, Y. Fabrication of symmetric supercapacitors based on MOF-derived nanoporous carbons. *J. Mater. Chem. A* **2014**, 2, 19848–19854.

(8) Liu, G. N.; Zhao, R. Y.; Xu, R. D.; Zhang, X.; Tang, X. N.; Dan, Q. J.; Wei, Y. W.; Tu, Y. Y.; Bo, Q. B.; Li, C. C. A novel tetranuclear copper(I) iodide metal-organic cluster Cu_4I_4(Ligand)(5) with highly selective luminescence detection of antibiotic. *Cryst. Growth Des*. **2018**, 18, 5441–5448.

(9) Liu, G. N.; Xu, R. D.; Zhao, R. Y.; Zhao, R. Y.; Sun, Y. Q.; Bo, Q. B.; Duan, Z. Y.; Li, Y. H.; Wang, Y. Y.; Wu, Q.; Li, C. C. Hybrid copper iodide cluster-based pellet sensor for highly selective optical detection of *o*-nitrophenol and tetracycline hydrochloride in aqueous solution. *ACS Sustain. Chem. Eng*. **2019**, 7, 18863–18873.

(10) Li, L.; Zou, J. Y.; You, S. Y.; Liu, Y. W.; Cui, H. M.; Zhang, S. W. A dual luminescent chemosensor derived from a europium(III) metal-organic framework for quantitative detection of phosphate anions and acetylacetone in aqueous solution. *Dyes. Pigments* **2020**, 173, 108004.

(11) Bradshaw, D.; El-Hankari, S.; Lupica-Spagnolo, L. Supramolecular templating of hierarchically porous metal–organic frameworks. *Chem. Soc. Rev.* **2014**, 43, 5431–5443.

(12) Cui, Y. J.; Yue, Y. F.; Qian, G. D.; Chen, B. L. Luminescent functional metal-organic frameworks. *Chem. Rev.* **2012**, 112, 1126–1162.

(13) Allendorf, M. D.; Bauer, C. A.; Bhakta, R. K.; Houk, R. J. T. Luminescent metal-organic frameworks. *Chem. Soc. Rev.* **2009**, 38, 1330–1352.

(14) Wang, K. C.; Lin, Z. E.; Huang, S.; Sun, J.; Zhang, Q. H. Microporous Metal-organic frameworks based on zinc clusters and their fluorescence enhancements towards acetone and chloroform. *Eur. J. Inorg. Chem.* **2016**, 21, 3411–3416.

(15) Park, K. S.; Ni, Z.; Cote, A. P.; Choi, J. Y.; Huang, R. D.; Uribe-Romo, F. J.; Chae, H. K.; O'Keeffe, M.; Yaghi, O. M. Exceptional chemical and thermal stability of zeolitic imidazolate frameworks. *P. Natl. Acad. Sci. USA* **2006**, 103, 10186–10191.

(16) Lan, Y. Q.; Li, S. L.; Fu, Y. M.; Du, D. Y.; Zang, H. Y.; Shao, K. Z.; Su, Z. M.; Fu, Q. Syntheses, structures, and luminescent properties of zinc(II) and cadmium(II) coordination complexes based on different (pyridyl)imidazole derivatives and 1,4-benzenedicarboxylate. *Cryst. Growth. Des.* **2009**, 9, 1353–1360.

(17) Song, J.; Duan, B. F.; Lu, J. F.; Wu, R.; Du, Q. C. Hydrothermal synthesis of three zinc(II) coordination polymers from 0D to 2D: synthesis, structure, luminescence properties and effect of auxiliary ligand on their structural architectures. *J. Mol. Struct.* **2019**, 1195, 252–258.

(18) Yam, V. W. W.; Lo, K. K. W. Luminescent polynuclear d^{10} metal complexes. *Chem. Soc. Rev.* **1999**, 28, 323–334.

(19) Wang, K. Y.; Ding, D.; Sun, M.; Cheng, L.; Wang, C. Effective and rapid adsorption of Sr^{2+} ions by a hydrated pentasodium cluster templated zinc thiostannate. *Inorg. Chem.* **2019**, 58, 10184–10193

(20) Wang, K. Y.; Feng, M. L.; Huang, X. Y.; Li, J. Organically directed heterometallic chalcogenidometalates containing group 12(II)/13(III)/14(IV) metal ions and antimony(III). *Coord. Chem. Rev*. **2016**, 322, 41–68.

(21) Jin, F.; Pan, C. Y.; Zhang, W. X.; Sun, L.; Hu, X. Y.; Liao, R. B.; Tao, D. L. Enhanced two-photon excited fluorescence of mercury complexes with a conjugated ligand: effect of the central metal ion. *J. Lumin.* **2016**, 172, 264–269.

(22) Yin, H. Q.; Yin, X. B. Metal-organic frameworks with multiple luminescence emissions: designs and applications. *Acc. Chem. Res*. **2020**, 53, 485–495.

(23) Liu, J. Q.; Wu, J.; Li, F. M.; Liu, W. C.; Li, B. H.; Wang, J.; Li, Q. L.; Yadave, R.; Kumar, A. Luminescent sensing from a new Zn(II) metal-organic framework. *Rsc Advances* **2016**, 6, 31161–31166.

(24) Chen, X. L.; Cui, H. L.; Yang, H.; Liu, L.; Wang, X.; Ren, Y. X.; Wang, J. J.; Han, B. A zinc(II) coordination polymer based on a polycarboxylate ligand: synthesis, crystal structure, photoluminescence and photocatalysis. *Chin. J. Struct. Chem*. **2019**, 38, 2148–2154.

(25) Li, J. D.; Bai, C.; Hu, H. M.; Yang, Z. H.; Xue, G. L. Solvothermal syntheses, crystal structures and luminescence properties of Zn(II) coordination compounds based on imidazophenanthroline carboxylate derivative ligand. *J. Solid State Chem.* **2019**, 277, 1–8.